Electronic Supplementary Information

Constructing all Zero-dimensional $CsPbBr_3$/CdSe Heterojunction for Highly Efficient Photocatalytic CO_2 Reduction

Guilin Yin,[a] Xiaosi Qi,[a] Yanli Chen,[a] Qiong Peng,[a] Xingxing Jang,[b] Qinglong Wang,[*c] Wenhua Zhang,[*d] Xiu Gong,[*a]

[a]College of Physics, & Guizhou Province Key Laboratory for Optoelectronic Technology and Application, Guizhou University, Guiyang 550025, China

[b]College of Chemistry and Environmental Engineering, Shenzhen University, Shenzhen, Guangdong 518060, China

[c]National & Local Joint Engineering Research Center for Applied Technology of Hybrid Nanomaterials, Henan University, Kaifeng 475004, China

[d]Yunnan Key Laboratory of Carbon Neutrality and Green Low-carbon Technologies, School of Materials and Energy, Yunnan University, Kunming 650500, China.

*Corresponding author.

E-mail: xgong@gzu.edu.cn; qlwang2021@163.com; wenhuazhang@ynu.edu.cn;

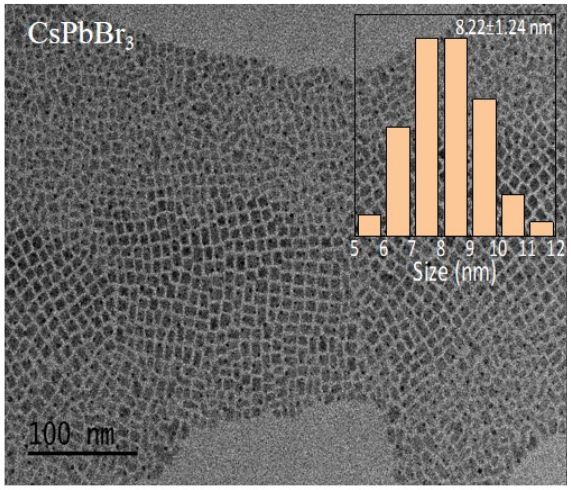

Fig. S1 TEM image of $CsPbBr_3$ QDs (size: 8.2±1.2 nm) Insets are corresponding histogram of the size distribution.

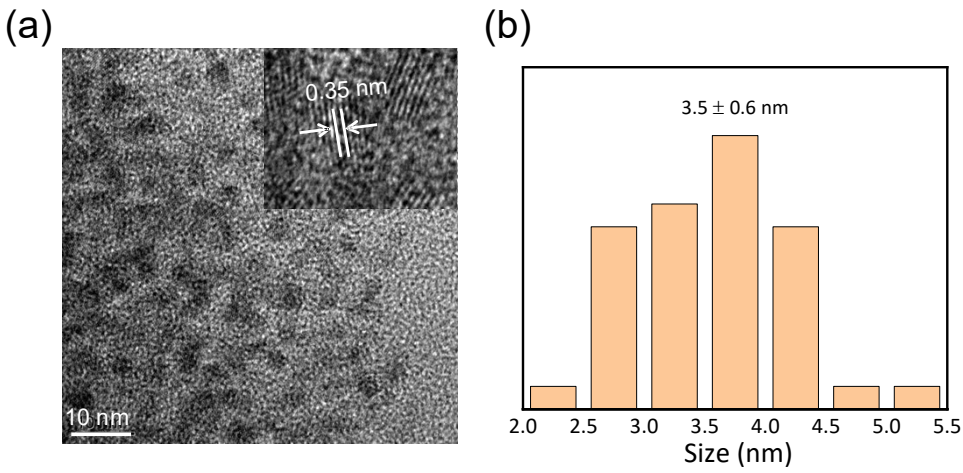

Fig. S2 (a) TEM images of CdSe QDs; (b) The average sizes of CdSe QDs.

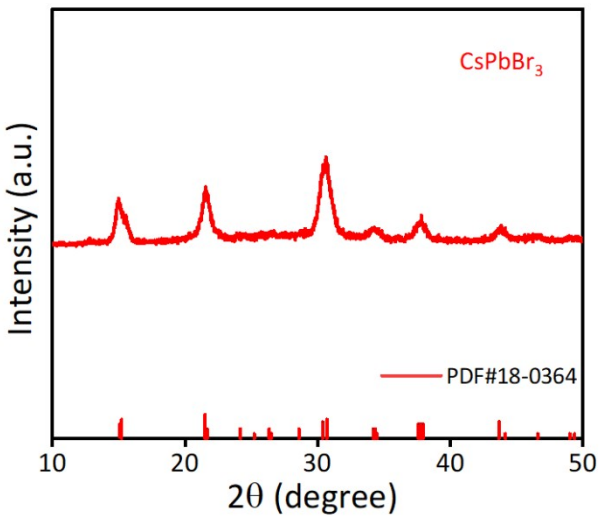

Fig. S3 XRD patterns of the $CsPbBr_3$.

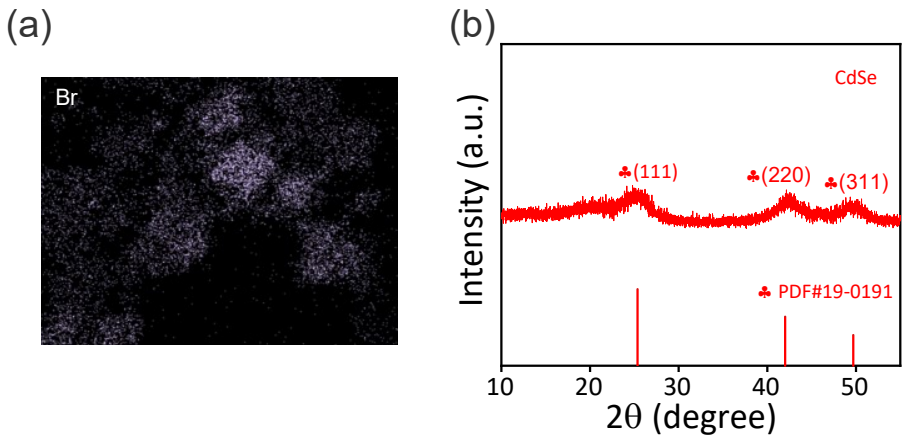

Fig. S4 (a) Br element mapping of $CsPbBr_3$/CdSe heterojunction. (b) XRD patterns of the CdSe QDs.

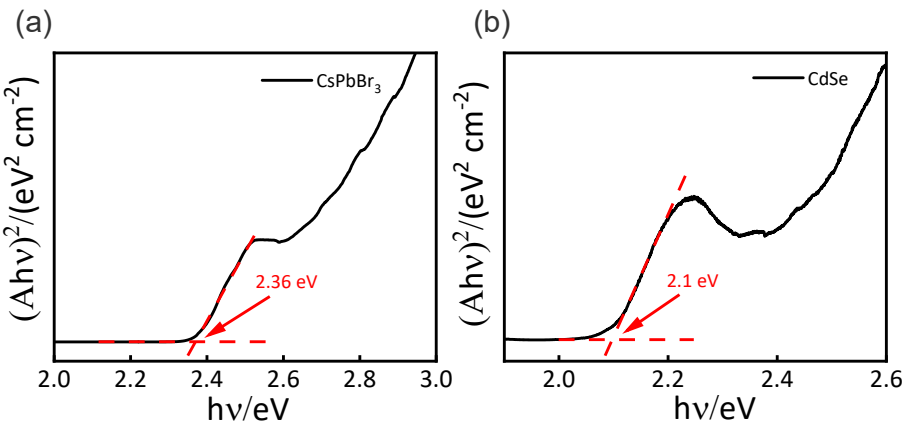

Fig. S5 (a) Tauc plot of the prepared $CsPbBr_3$ and (b) CdSe QDs for determining their optical bandgaps.

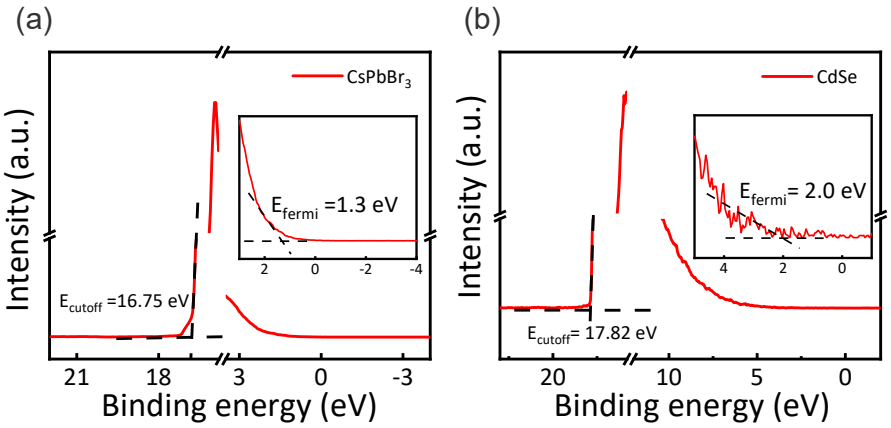

Fig. S6 UPS spectra of $CsPbBr_3$ QDs and CdSe QDs.

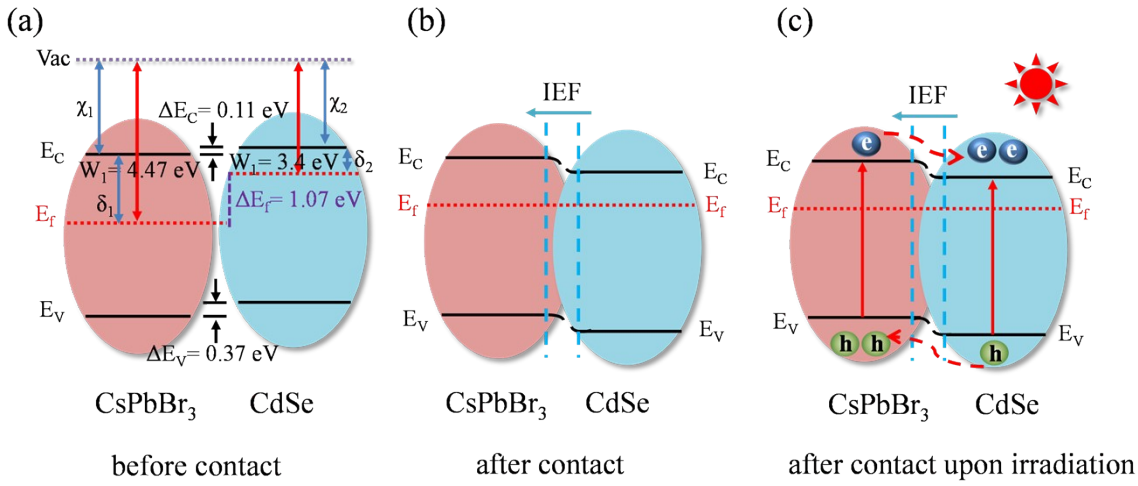

Fig. S7 Illustration of band structures of $CsPbBr_3$/CdSe heterojunction.

Fig. S7a illustrated that the electrons in CdSe with higher Fermi levels would spontaneously diffuse to $CsPbBr_3$ with lower Fermi levels to achieve an equalization of their Fermi levels. The simultaneously generated built-in IEF facilitates the separation of photogenerated electrons and holes. Moreover, the band edge of CdSe will bend upward owing to the loss of electrons, while that of $CsPbBr_3$ will inversely bend downward. Upon light illumination, as shown in Fig S7c, the staggered band alignment can result in type-II heterojunction interfaces, which would lead to the opposite electron transfer routes. [1-3]

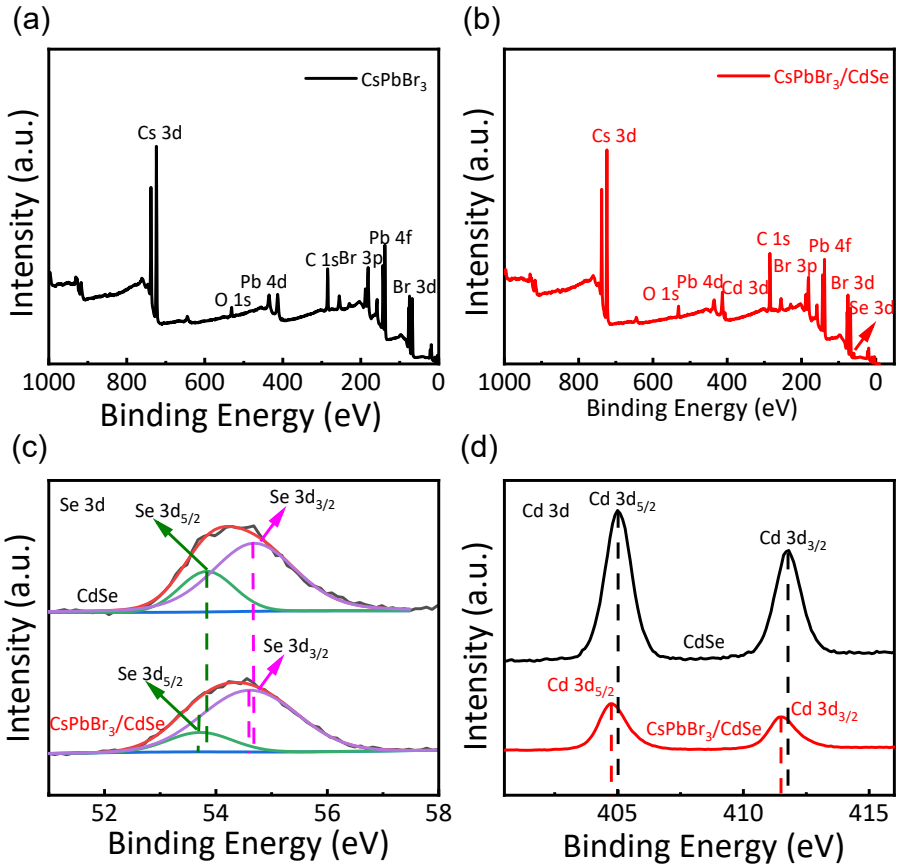

Fig. S8 Survey XPS spectra of $CsPbBr_3$ QDs (a) and $CsPbBr_3$/CdSe heterojunction (b); XPS spectra of $CsPbBr_3$/CdSe heterojunction: (c) Se 3d spectra; (d) Cd 3d spectra

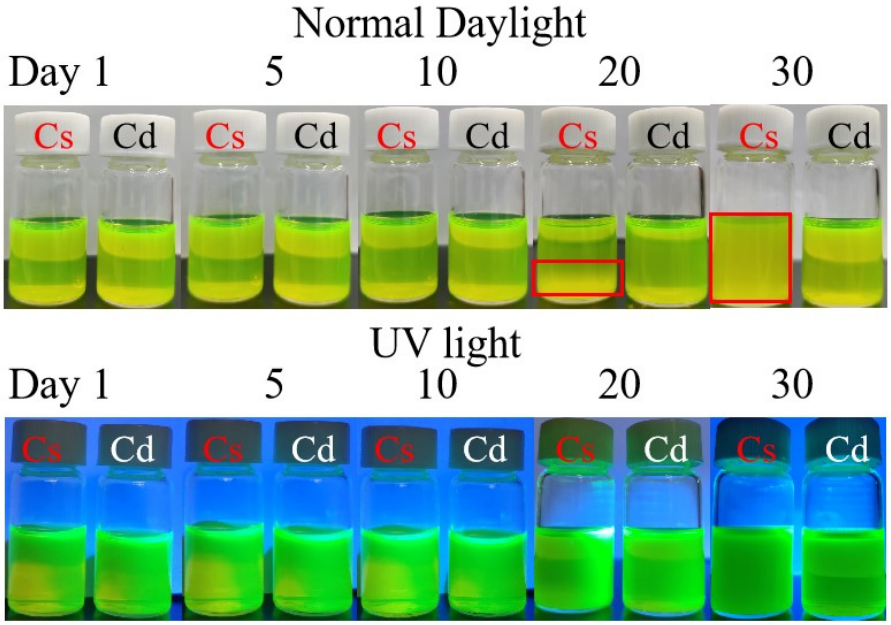

Fig. S9 Photographs evolution of the $CsPbBr_3$ and $CsPbBr_3$/CdSe heterojunction in normal daylight and UV light after aging for 30 days. The same concentration of both $CsPbBr_3$ QDs and $CsPbBr_3$/CdSe heterojunction.

The $CsPbBr_3$/CdSe solution exhibited more clarification and high luminescence brightness, while the control $CsPbBr_3$ QDs solution was relatively turbidity, indicating severe degradation and aggregation of QDs due to the OA surface ligand loss or damage after aging for 30 days.[4] These results clearly show that the heterojunction $CsPbBr_3$/CdSe heterojunction demonstrated has higher stability than single $CsPbBr_3$ QDs.

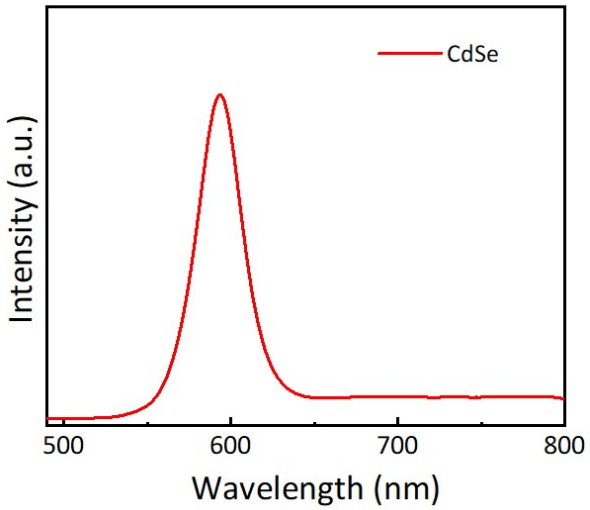

Fig. S10 PL spectra of CdSe QDs.

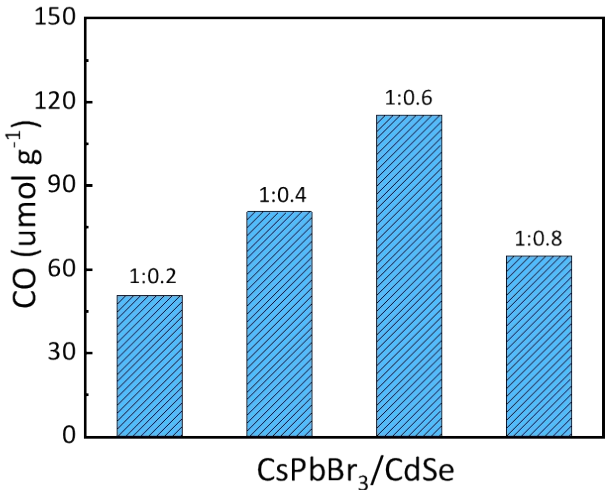

Fig. S11 Photocatalytic CO_2 reduction by using $CsPbBr_3$/CdSe heterojunction with various mole ratios of $CsPbBr_3$ and CdSe after 3 h of photocatalytic reaction.

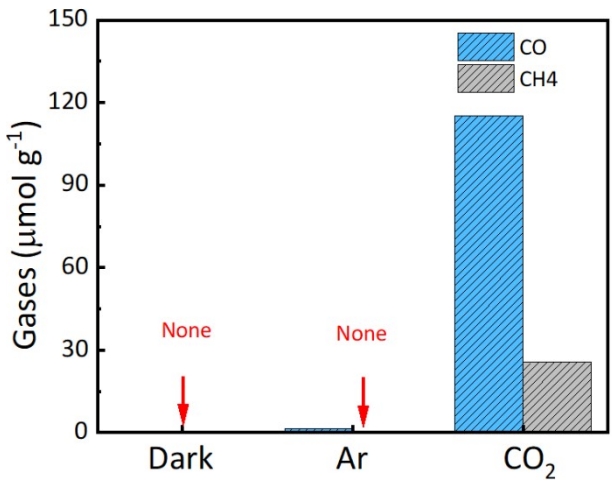

Fig. S12 Control photocatalytic tests using $CsPbBr_3$/CdSe as catalysts under CO_2 atmosphere with the dark condition; under Ar atmosphere with light irradiation; and under CO_2 atmosphere with light irradiation after 3h.

The control photocatalytic experiments show that the traces of CO were detected under Ar atmosphere (Fig. S10), which may be related to the partial photooxidation of ethyl acetate. [5-7]

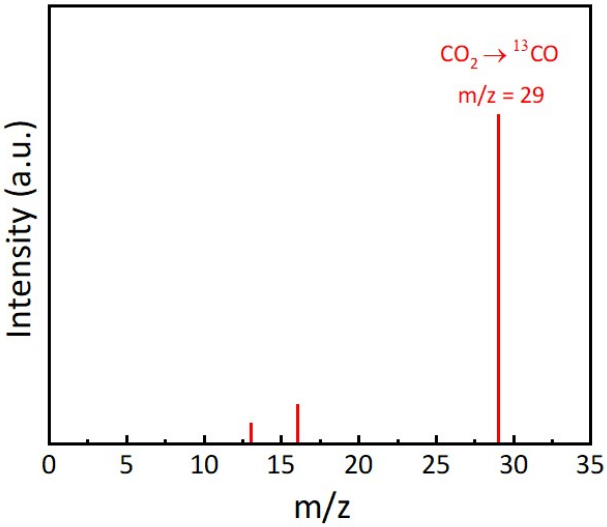

Fig. S13 Mass spectra from ^{13}CO (m/z=29) produced over $CsPbBr_3$/CdSe catalyst in the photocatalytic reduction of $^{13}CO_2$.

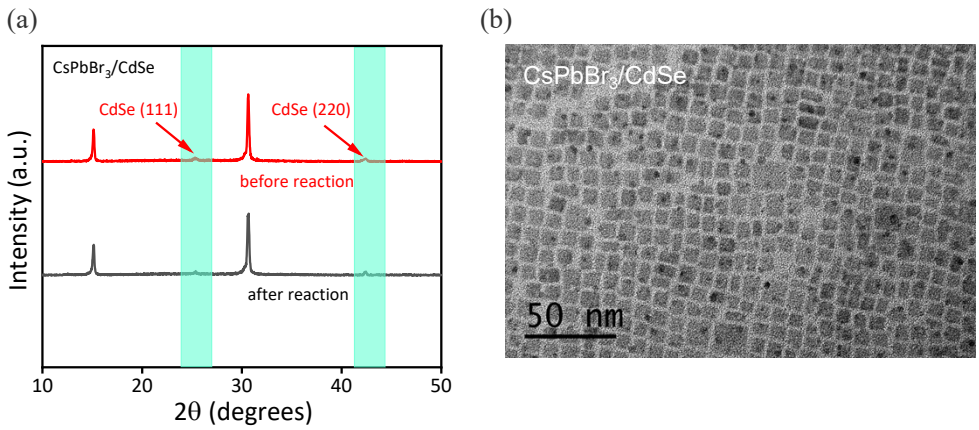

Fig. S14 (a) XRD patterns of $CsPbBr_3$/CdSe QDs before and after the photocatalytic reaction; (b) TEM image of $CsPbBr_3$/CdSe QDs after the photocatalytic reaction. The $CsPbBr_3$/CdSe QDs were maintained after three catalytic runs.

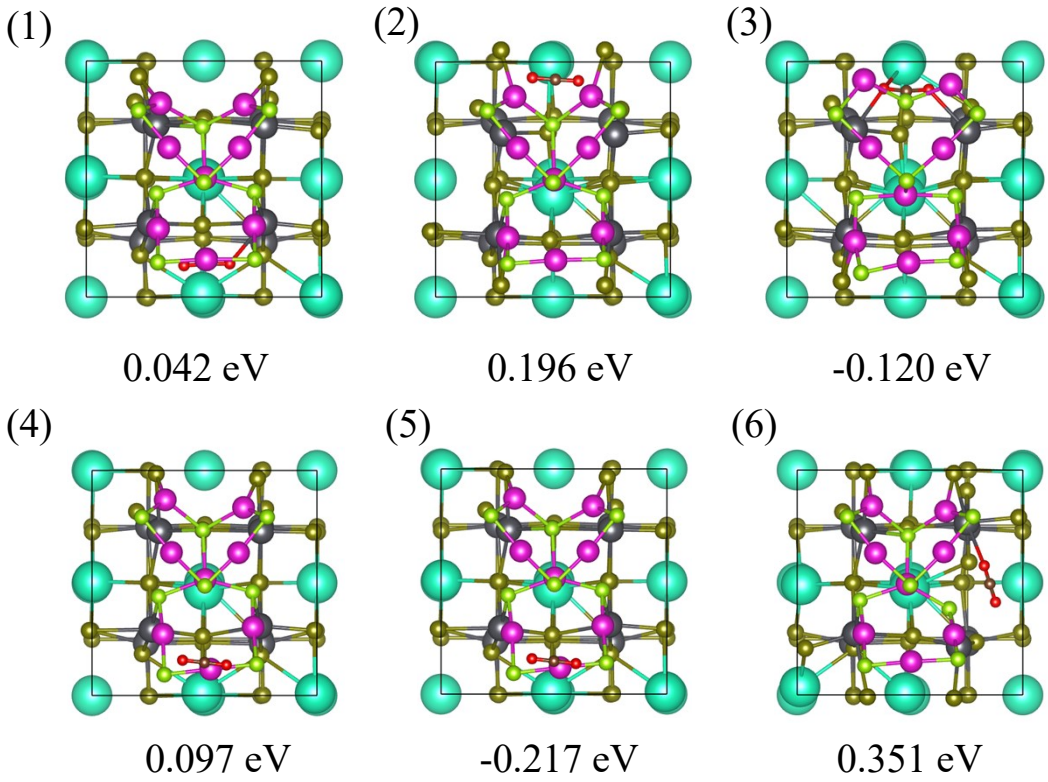

Fig. S15 The six adhesive sites for CO_2 onto the $CsPbBr_3$/CdSe heterojunction and corresponding adhesive energies.

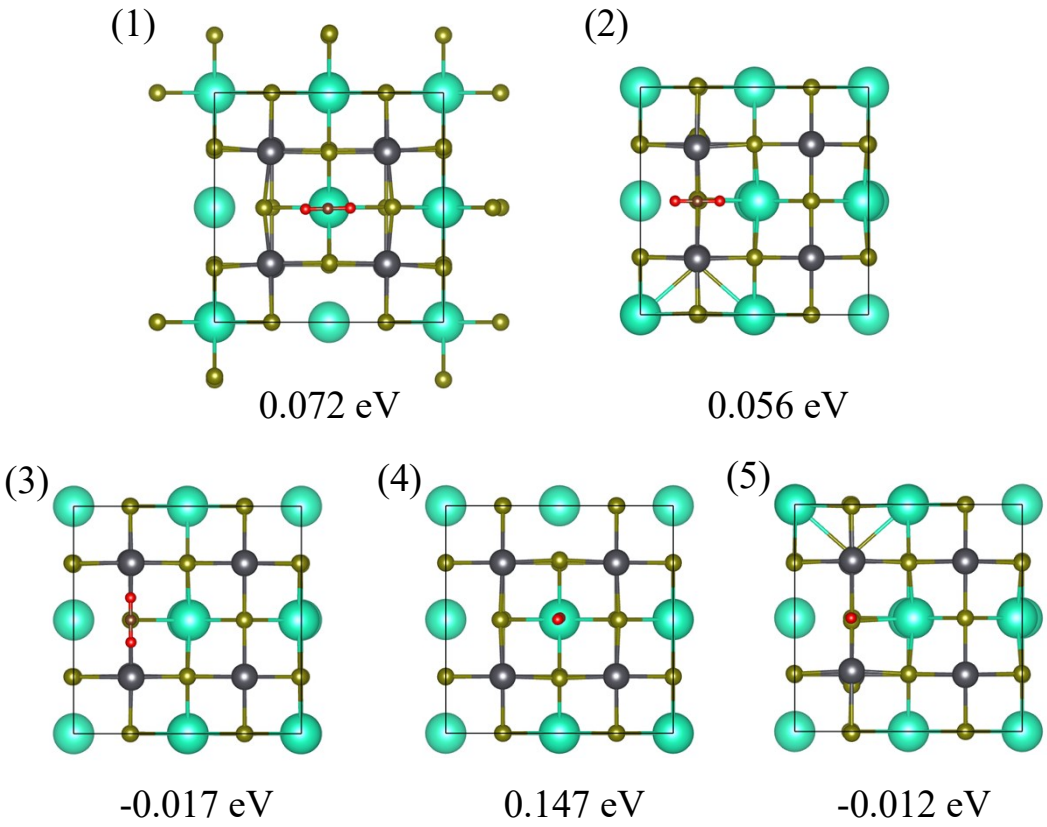

Fig. S16 The five adhesive sites for CO_2 onto the $CsPbBr_3$ QDs and corresponding adhesive energies.

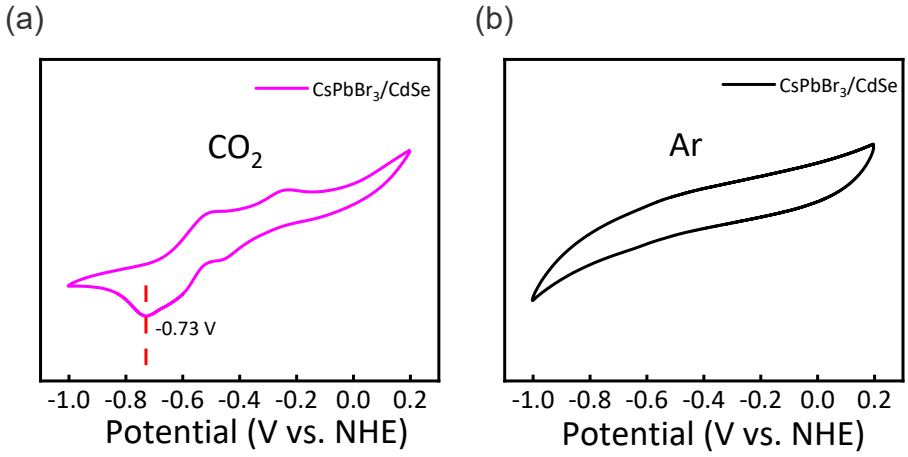

Fig. S17 Cyclic voltammogram curve of $CsPbBr_3$/CdSe heterojunction photocatalyst under CO_2 atmosphere and Ar atmosphere, respectively.

Table S1 Adhesive energies from different adhesive sites for CO_2 onto the $CsPbBr_3$ QDs and $CsPbBr_3$/CdSe heterojunction.

Site	$CsPbBr_3$	$CsPbBr_3$/CdSe
1	0.072 eV	0.042 eV
2	0.056 eV	0.196 eV
3	-0.017 eV	-0.120 eV
4	0.147 eV	0.094 eV
5	-0.012 eV	-0.217 eV
6	--	0.351 eV

Table S2 A summary of the photocatalytic CO_2 reduction performances by metal halide perovskites photocatalysts.

Photocatalyst	Solvent	Light source	Products and Yield ($\mu mol\ g^{-1}\ h^{-1}$)			Refs.
			CO	CH_4	H_2	
$CsPbBr_3$/CdSe	Ethyl acetate/H_2O	300 W Xe lamp, 420 nm filter, 150 mW cm^{-2}	38.43	8.52	/	This work
$CsPbBr_3$/GO	Ethyl acetate	100 W Xe lamp, AM 1.5G filter	4.89	2.47	0.13	J. Am. Chem. Soc. 2017, 139, 5660
$CsPbBr_3$/BZNW/MRGO	CO_2/H_2O vapor	150 W Xe lamp, $\lambda > 420$ nm, 150 mW cm^{-2}	0.85	6.29	/	J. Mater. Chem. A 2019, 7,1 3762
$MAPbI_3$@PCN-221($Fe_{0.2}$)	Ethyl acetate or Acetonitrile/H_2O	300 W Xe lamp, 400 nm filter, 100 mW cm^{-2}	4.16	13.00	/	Angew. Chem. Int. Ed. 2019, 58, 9491
$CsPbBr_3$/MXene-20	Ethyl acetate	300 W Xe-lamp, $\lambda > 420$ nm	26.32	7.25	/	*J. Phys. Chem. Lett.* 2019, 10, 6590
$CsPbBr_3$@TiO-CN	Ethyl acetate/H_2O	300 W Xe lamp, 400 nm filter, 100 mW cm^{-2}	12.9	/	/	*RSC Adv.* 2019, 9, 34342
$CsPbBr_3$@g-C_3N_4	Ethyl acetate	300 W Xe lamp	2.08	22.82		*Dalton Trans.* 2019, 48, 14115
$CsPbBr_3$/UiO-66(NH_2)	Ethyl acetate/H_2O	300 W Xe lamp, $\lambda > 420$ nm	8.21	0.26	/	*Chem. Eng. J.* 2019, 358, 1287
$Co_{2\%}$@$CsPbBr_3$/Cs_4PbBr_6	H_2O solution	300 W Xe lamp, 400 nm filter,100 mW cm^{-2}	11.95	/	/	*ChemSusChem* 2019, 12, 4769
$CsPbBr_3$/Pd NS(600)	CO_2/H_2O vapor	150 W Xe lamp, λ >420 nm, 150 mW cm^{-2}	5.76	10.41	3.28	*ACS Appl. Energy Mater.* 2018, 1, 5083-5089
$CsPbBr_3$@ZIF-67	CO_2/H_2O vapor	100 W Xe lamp AM 1.5G, 150 mW cm^{-2}	0.77	3.51	/	*ACS Energy Lett.* 2018, 3, 2656
$CsPbBr_3$/a-TiO_2(20)	Ethyl acetate/isopropanol	150 W Xe lamp, AM 1.5G flter, 150 mW cm^{-2}	3.90	6.72	1.46	*Adv. Mater. Interfaces* 2018,

						1801015
Fe^{2+}: $CsPbBr_3$	Ethyl acetate/H_2O	450 W Xe-lamp,150 mW cm^{-2}	3.2	6.1	/	*J. Phys. Chem. Lett.* 2019, 10, 7965
$Cs_2AgBiBr_6$	Ethyl acetate	100 W Xe-lamp, AM 1.5G, 150 mW cm^{-2}	2.35	1.60	/	*Small* 2018, 14, 1703762
Cs_2SnI_6(1.0)/SnS_2	CH_3OH/H_2O	32 W UV lamp 305nm, 80.38 μW cm^{-2}	/	6.09	/	*J. Am. Chem. Soc.* 2019, 141, 13434
$Cs_3Bi_2I_9$	CO_2/H_2O vapor	32 W UV lamp 305nm, 80.38 μW cm^{-2}	7.76	1.49	/	*J. Am. Chem. Soc.* 2019, 141, 20434
$CsPbBr_3$	Ethyl acetate/H_2O	300 W Xe lamp, AM 1.5 G filter	4.3	1.5	0.1	*Chem. Eur. J.* 2017, 23, 9481

References

[1] Y. Zhang, Q. Wang, D. Liu, Q. Wang, T. Li and Z. Wang, Appl. Surf. Sci.，2020, 521, 146434.

[2] Q. Xu, L. Zhang, B. Cheng, J. Fan and J. Yu, Chem, 2020, 6, 1543-1559.

[3] S. Bai, J. Jiang, Q. Zhang and Y. Xiong, Chem. Soc. Rev., 2015, 44, 2893-2939.

[4] H. Yao, A. Lu, Z. Bai, J. Jiang, S. Qin, Chinese. Phys. B., 2022, **4**, 046106.

[5] J. Wang, J. Wang, N. Li, X. Du, J. Ma, C. He, Z. Li, ACS Appl. Mater. Interfaces., 2020, **12**, 31477-31485.

[6] Q. Wang, J. Wang, J. C. Wang, X. Hu, Y. Bai, X. Zhong and Z. Li, ChemSusChem, 2021, **14**, 1131-1139.

[7] L. Zhou, Y. F. Xu, B. X. Chen, D. B. Kuang and C. Y. Su, Small, 2018, **14**, 1703762.